J. Jpn. Soc. Soil Phys.
土壌の物理性
No. 90, p. 11～19（2002）

The effect of heterogeneous soil-water distribution on the TDR measurement of soil-water content

M. A. Mojid, Nobuo Toride and Hiroyuki Cho

Department of Agricultural Sciences, Saga University, Saga 840-8502, Japan

Abstract

This study investigated the shape of the TDR waveforms and compatibility of TDR support softwares to analyze the waveforms for dielectric constant, ε, to estimate volumetric water content, θ, in sands with heterogeneous distribution of water. When a dry layer was at the bottom, the waveform shifted upward due to reflection of the TDR pulse at the wet-dry interface before the final reflection of the pulse at the end of the sensor. The program algorithm incorrectly located the point of final reflection at the beginning of the dry sand layer when the water content of the dry layer, θ_{dry}, was less than $0.15\,m^3\,m^{-3}$. Selection of inflection points at the wet-dry interface resulted in underestimation of ε and θ. For $\theta_{dry}=0.22\,m^3\,m^{-3}$, the magnitude of the upward shift was not significant. The program then correctly determined the reflection point at the end of the sensor. Thickness of the bottom dry sand layer, L_{dry}, had no effect on the wave analysis. When the bottom layer was quite dry ($\theta_{dry}=0.05\,m^3\,m^{-3}$), the inflection point was always selected just after the pulse reflected back at the wet-dry sand interface regardless of L_{dry} values, resulting in underestimation of ε and θ. On the other hand, TDR always underestimated ε and θ when water contents were different between two rods of the sensor. The degree of underestimation was higher when the core wire of the sensor was in dry sand.

Key words : Time-domain reflectometry, soil-water distribution, longitudinal heterogeneity, transverse heterogeneity, wave form analysis

1. Introduction

Time-domain reflectometry (TDR) has become a widely used technique for measuring soil-water content, θ, since its introduction to measure the dielectric constant, ε, of soil (Davis and Chudobiak, 1975), and the development of a calibration equation between the dielectric constant and soil-water content (Topp *et al*., 1980). The technique is considered robust since it is almost unaffected by temperature, salinity and soil texture, and reliable over a wide range of soil-water condition within an accuracy of $\pm 0.01\,m^3\,m^{-3}$ of water content (Topp *et al*, 1980).

Topp *et al*. (1982) showed both theoretically and experimentally that TDR measures the average dielectric constant of the sampled volume using layered soil. However, Nadler *et al*. (1991) showed that a heterogeneous soil profile with wet soil overlaid dry soil reduced the accuracy of determining ε by TDR. Dasberg and Hopmans (1992) also evaluated the effects of layered profile on the TDR-measured ε for sandy loam and clay loam soils using 20 cm long 2-wire and 3-wire sensors. They obtained significantly lower ε when wet soil overlaid dry soil. A distinct reflection of TDR pulse from the wet-dry soil interface caused difficulty to identify the final point of reflection of the pulse from the end of the sensor.

Hokett *et al*. (1992) studied water content heterogeneity in the transverse direction to the TDR sensor by inserting one wire of a two-wire sensor in a dry sand and the other wire in a wet sand ; the dry and wet sands were separated by

either an artificially made air- or water-filled crack. They reported that TDR measurement was significantly influenced by the dry sand and ε was underestimated. Air-filled crack caused underestimation in ε only slightly in dry sand but significantly in wet sand. The effect of water-filled cracks was small in both dry and wet sands.

The main current of the TDR pulse transmits through the wire of the sensor connected to the core of the coaxial cable. Intensity of electrical potential is also higher around this wire than the other wire connected to the shield. As a result, the transverse heterogeneous water distribution in a soil would affect TDR-measured ε depending on the type of the sensor wire in dry and wet soils. Hokett *et al*. (1992) did not consider this factor in their study.

A heterogeneous soil-water distribution is often encountered in practice, such as in the root zone of layered soils, and during infiltration and evaporation processes in unsaturated soils. We decided to further investigate the shape of the TDR-waveforms for various different combinations of water content and thickness of dry and wet soil layers, and compatibility of TDR-support softwares to analyze these waveforms. The objectives of this study were : (1) to investigate the effects of a dry soil layer with different water content and thickness at the end of a sensor on the TDR waveform, (2) to evaluate the comparative performance of the software algorithms to identify two reflection points on the waveform, and (3) to evaluate the response of the core and shield wires of a 2-wire sensor for transverse heterogeneous soil-water distributions and its effect on TDR-measured dielectric constant.

2. Materials and Method

We conducted five different experiments using Tottori dune sand, Japan. The first four experiments were designed to evaluate the effect of longitudinal heterogeneity on TDR measurements : water contents were heterogeneous along the sensor. Fifth experiment was for transverse heterogeneity : water contents were different between two rods of the sensor. Summaries of these experiments are given in Tables 1 and 2. We used TDR sensors of Easy Test, Ltd., Poland consisting of 2 wires of 0.1 m in length ; the diameter and spacing between the wires were 1 mm and 5 mm, respectively. There was an 8 cm epoxy transition between the wires of the sensor and the coaxial cable to hold the cable and sensor wires firmly. One wire of the sensor was connected to the core of the coaxial cable, and the other wire was connected to the shield of the coaxial cable. TDR sensors were connected with a Tektronix 1502 C cable tester of Tektronix Ltd. using a SDMX 50 ohm coaxial multiplexer. The TDR waveforms were analyzed with a CR10X datalogger with PC208W program of the Campbell Scientific Ltd., and WinTDR99 program of Or *et al*. (1999) as well.

A 10 cm high acrylic soil column with 5 cm inner diameter having a ceramic plate at the bottom was used in the first four experiments. Fig.1 shows water content profiles for these experiments. The column consisted of several rings depending on the water content profile. Expt.1 compared a wet and dry layered column and a uniform column, both having same average water content ($\theta = 0.195\ m^3\ m^{-3}$). For Expt. 1.1, the bottom 5 cm of the column was relatively dry ($\theta_{dry} = 0.10\ m^3\ m^{-3}$) and the top 5 cm was relatively wet ($\theta_{wet} = 0.29\ m^3\ m^{-3}$). Expt.2 was conducted for three different water contents at the bottom 5 cm layer ($\theta_{dry} = 0.05$, 0.15, 0.25 $m^3\ m^{-3}$) having a same water content ($\theta_{wet} = 0.29\ m^3\ m^{-3}$) at the top 5 cm layer. Expt.3 was for different thickness of the bottom dry layer ($\theta_{dry} = 0.05\ m^3\ m^{-3}$) ranging 0 to 5 cm below the wet layer ($\theta_{wet} = 0.29\ m^3\ m^{-3}$). Expt.4 was similar to Expt.3 but the bottom layer is relatively wet ($\theta_{dry} = 0.22\ m^3\ m^{-3}$). In all experiments, the soil column was filled uniformly with an average bulk density of $1.66\ Mg\ m^{-3}$. The wet and dry sands were separated using a thin laboratory film to prevent vertical flow. Equally spaced four TDR sensors were inserted vertically in

Table 1 Experimental details for the longitudinal heterogeneous water distributions (Expt. 1–Expt. 4) with average gravimetric and TDR-measured dielectric constants (ε_{grav} and ε_{TDR}) and soil-water contents (θ_{grav} and θ_{TDR})

Expt. No.	Measurement No.	Soil layer arrangement				ε_{grav}	ε_{TDR}	θ_{grav}	θ_{TDR}
		L_{wet} (cm)	θ_{wet}	L_{dry} (cm)	θ_{dry}				
1	1	5	0.29	5	0.10	9.83	7.55	0.195	0.138
	2	10	0.195	—	—	9.82	9.78	0.195	0.184
2	1	5	0.29	5	0.05	8.45	7.92	0.170	0.140
	2	5	0.29	5	0.15	11.33	10.18	0.220	0.192
	3	5	0.29	5	0.25	14.67	14.83	0.270	0.273
3	1	10	0.29	—	—	16.21	15.97	0.291	0.291
	2	9	0.29	1	0.05	14.46	12.58	0.267	0.236
	3	8	0.29	2	0.05	12.74	10.80	0.242	0.204
	4	7	0.29	3	0.05	11.20	9.17	0.218	0.172
	5	6	0.29	4	0.05	9.71	8.11	0.193	0.150
	6	5	0.29	5	0.05	8.40	6.79	0.169	0.121
4	1	10	0.29	—	—	15.76	15.78	0.285	0.288
	2	9	0.29	1	0.22	15.25	14.79	0.278	0.272
	3	8	0.29	2	0.22	14.75	15.02	0.271	0.276
	4	7	0.29	3	0.22	14.25	14.50	0.264	0.268
	5	6	0.29	4	0.22	13.76	13.36	0.257	0.249
	6	5	0.29	5	0.22	13.28	12.98	0.250	0.243

the columns from the soil surface. The TDR waveforms, first derivatives of the waveforms, ε and θ were measured for all experiments. An average of five measurements was recorded for each sensor. Note that five successive measurements of each sensor resulted in almost identical results and, furthermore, there was no remarkable difference between these sensors. We therefore assumed overall averages of four sensors could represent reliable ε and θ values.

For the transverse heterogeneity (Expt.5), a 10 cm long plastic column with 1.5 cm inner diameter was partitioned longitudinally into two approximately equal portions with a thin adhesive tape. The two portions of the column were filled with sands of two different water contents. One TDR sensor was inserted in this column keeping the core and shield wires in its two portions. The measurement of ε and θ was repeated by interchanging the mutual positions of the two wires of the sensor in the sample. Different sampling volumes of the dry

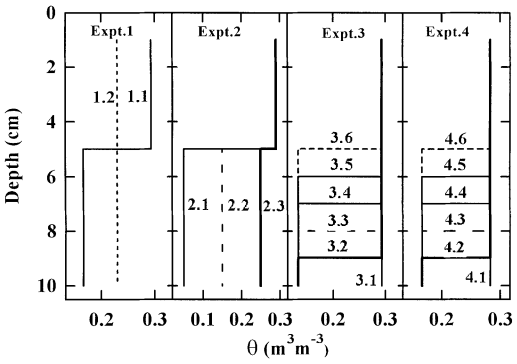

Fig. 1 Soil water content profiles for the longitudinal heterogeneous conditions (Expt. 1–Expt. 4).

and wet sands were also measured by changing the relative position of the sensor from the partition (No. 9–11 in Table 2). After the measurements, the average water contents in the two portions of the column were measured gravimetrically. We note that we failed to determine exact water contents of wet and dry

Table 2 Experimental details for the transverse heterogeneous water distributions (Expt. 5) with average gravimetric and TDR-measured water contents (θ_{grav} and (θ_{TDR}), and corresponding dielectric constants (θ_{grav} and (θ_{TDR}) based on the Topp equation

No.	θ_{grav}	ε_{grav}	Arrangement of wires		θ_{TDR}	ε_{TDR}
			Core wire	Shield wire		
1	0.272	15.49	wet	dry	0.184	10.01
			dry	wet	0.135	7.44
2	0.317	18.73	wet	dry	0.247	13.79
			dry	wet	0.210	11.47
3	0.224	12.36	wet	dry	0.177	9.63
			dry	wet	0.142	7.82
4	0.186	10.13	wet	dry	0.115	6.54
			dry	wet	0.107	6.19
5	0.233	12.92	wet	dry	0.165	8.99
			dry	wet	0.151	8.26
6	0.115	6.52	wet	dry	0.102	5.97
			dry	wet	0.083	5.18
7	0.160	8.71	wet	dry	0.141	7.74
			dry	wet	0.097	5.76
8	0.300	17.50	wet	dry	0.241	13.44
			dry	wet	0.224	12.35
9	0.238	13.22	wet	dry	0.142	7.80
			dry	wet	0.121	6.82
10	0.238	13.22	wet	dry	0.151	8.26
			dry	wet	0.128	7.14
11	0.238	13.22	wet	dry	0.225	12.37
			dry	wet	0.188	10.24
12	0.300	17.50	wet	air	0.100	5.89
			air	wet	0.069	4.64

sands in Expt.5. Total twelve measurements were carried out for different combinations of water contents and sampling volumes. In one measurement, one of the wires was kept in air (No. 12).

3. TDR Principle to Measure Soil-Water Content

TDR cable tester sends a high frequency electromagnetic pulse through a coaxial cable to a sensor. The launched pulse reflects back when it encounters a change in impedance on its path of travel. The reflected pulses superimpose on the launched pulse and are displayed as a waveform in time. The horizontal axis represents the distance from the output point of the TDR cable tester. The vertical axis provided the impedance of the TDR pulse. The shape of the waveform on the horizontal axis up to the beginning of the sensor wire is the characteristic feature of a particular sensor. The TDR waveform shifts up or down at any point due to the lower or higher dielectric constant of the surrounding material than for the previous point (Tektronix, 1990).

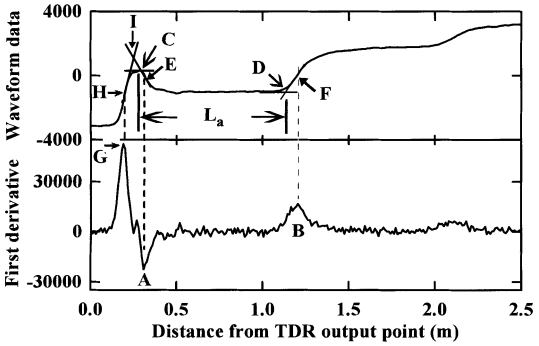

Fig. 2 A TDR waveform and its first derivative in distilled water.

Figure 2 shows a TDR waveform and its first derivative in distilled water. Initial and final points of reflection of the launched TDR pulse from the starting and end points of the sensor, denoting C (or I) and D in Fig. 2, respectively, are utilized for the interpretation of dielectric constant. The dielectric constant of the soil controls the distance between these points (Lorrain and Corson, 1970). Substantial efforts have been made to locate these two points (Baker and Allmaras, 1990 ; Heimovaara and Bouten, 1990 ; Evett, 1998 ; Or *et al*., 1999) since they are not clearly defined on the waveform as can be seen in Fig. 2. Virtually, all TDR-support softwares identify these points more or less in a similar way by utilizing the first

derivative of the waveform. In PC208W, an approximate location of the initial reflection is defined by the electrical length of the cable between the cable tester and the sensor, and a correction factor of the sensor. The point of initial reflection C is located at the intersection of a horizontal line passing through the global maximum of the waveform and a line tangent drawn to the inflection point of the waveform (point E) determined by its lowest first derivative (point A). In WinTDR99, the point of initial reflection is defined by the intersection of two tangent lines, which are drawn at the two inflection points on the waveform (points H and E). H is located at the highest positive peak of the first derivative (point G) before the first peak of the waveform. The point of initial reflection defined in WinTDR99 (point I) does not differ significantly from C ; both C and I provide comparable dielectric constants. The final point of reflection D is located in both programs at the intersection of a horizontal line passing through the global minimum of the waveform or a regression line through a range of points around this minimum and a line tangent drawn at the inflection point of the waveform after the minimum (point F). The inflection point F is located at the point of the highest first derivative of the waveform after the global minimum (point B).

The distance between the initial and final points of reflections is the apparent length of travel of the pulse through the sensor L_a (m). The average dielectric constant, ε, of the surrounding medium is calculated from the electrodynamic relationship as

$$\varepsilon=\left(\frac{L_a}{L_s\nu_p}\right)^2 \quad (1)$$

where L_s is the length of the sensor (0.1 m in this study), and ν_p is a ratio of the velocity of the TDR pulse in a medium to that in free space, which is obtained from TDR setting. The volumetric soil-water content, θ, is related to ε each other by the equations of Topp *et al.* (1980) :

$$\theta=-5.3\times10^{-2}+2.92\times10^{-2}\varepsilon-5.5\times10^{-4}\varepsilon^2+4.3\times10^{-6}\varepsilon^3 \quad (2)$$

$$\varepsilon=3.03+9.3\theta+146.0\theta^2-76.7\theta^3 \quad (3)$$

The gravimetrically measured θ_{grav} agreed well with the TDR-estimated θ_{TDR} based on the TDR-measured ε_{TDR} using Eq.(2) for the Tottori dune sand with an accuracy of $\pm0.02\,m^3\,m^{-3}$ of soil-water content. We therefore assumed that the dielectric constant based on θ_{grav} using Eq. (3), denoting ε_{grav}, represented a true dielectric constant for the comparison with the TDR-measured ε_{TDR}.

4. Results and Discussion

4. 1 Longitudinal Heterogeneity along the Sensor

Fig. 3 shows two waveforms for a wet-dry sand combination (Expt.1.1) and a uniformly wet sand (Expt.1.2), both having same average water content of $\theta=0.195\,m^3\,m^{-3}$. The first derivatives of these waveforms are also displayed in this figure to distinguish the final points of inflection on the waveforms. For the uniform sand, as similar to Fig. 2, the TDR pulse reflected back at the end of the sensor (point A in Fig.3) resulting in the inflection point at B.

In case of the wet-dry sand combination, the major portion of the TDR pulse reflected back and moved up considerably after traveling in

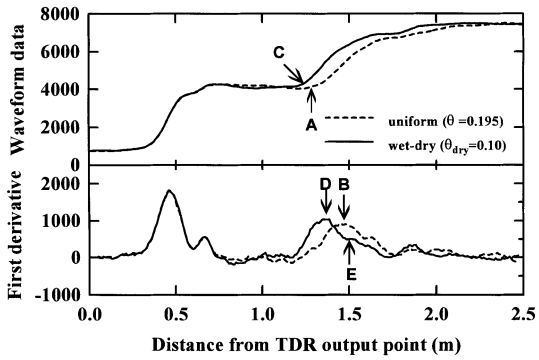

Fig. 3 TDR waveforms and their first derivatives for a wet-dry sand combination and a uniformly wet sand both having same average water content of ($\theta=0.195\,m^3\,m^{-3}$ (Expt. 1).

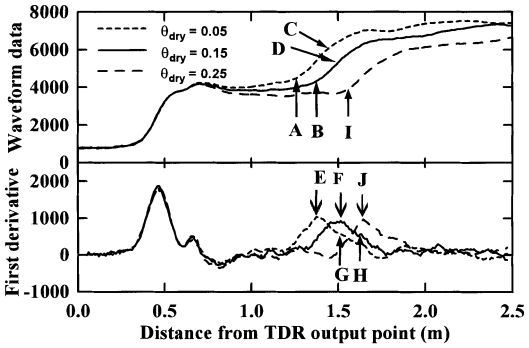

Fig. 4 TDR waveforms and their first derivatives for three different water contents of the bottom dry sand layer, (θ_{dry} (Expt. 2).

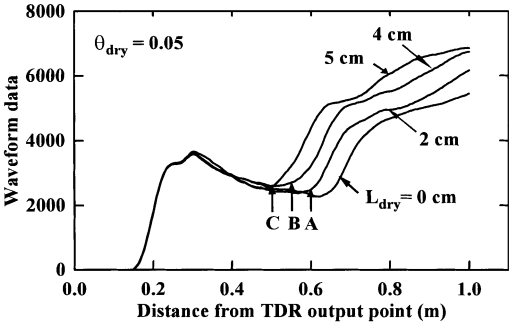

Fig. 5 TDR waveforms for four different thickness of the dry sand layer, *L*dry, with (θ_{dry} = 0.05 $m^3 m^{-3}$ (Expt. 3).

the wet sand while the remaining portion traveled in the dry sand until it reflected back at the end of the sensor. The approximate reflection point at the wet-dry interface is point C in Fig.3. The first inflection point of the waveform after the interface was identified by a distinct positive peak on the first derivative at D. The second reflection corresponding to the end of the sensor should be at A since the average water content was identical to the uniformly wet sand. Since the reflection of the pulse at the end of the sensor was very small, there was no any distinct peak on the first derivative for the inflection point. From close observation of Fig.3, a small upward shift of the first derivative at E might correspond to the inflection point after the reflection of the end of the sensor.

The programs drew a tangent line at D for the wet-dry layers to determine the final reflection point while point B was used for the uniformly wet sand. This interpretation of the final reflection point C in the wet-dry combination underestimated the travel path of the pulse L_a of Eq.(1), resulting in underestimation of ε and θ according to Eqs.(1) and (2), respectively. As shown in Table 1, θ_{grav} and θ_{TDR} for the wet-dry combination were 0.195 $m^3 m^{-3}$ and 0.138 $m^3 m^{-3}$, respectively. For the uniformly wet sand, ε_{TDR} and θ_{TDR} agreed well with ε_{grav} and θ_{grav}, respectively, showing the applicability of Eq.(2) for the Tottori dune sand.

The water content of the bottom dry sand layer, θ_{dry}, was an important factor that governed the performance of the programs. Fig. 4 displays waveforms and their first derivatives for three different θ_{dry} values in Expt.2. The reflected pulse moved up considerably after major reflection at the wet-dry sand interface (A and B) and resulted in waveforms without the reflected pulse from the end of the sensor (around C and D) for θ_{dry} = 0.05 and 0.15 $m^3 m^{-3}$. Accordingly, the major peak of the first derivative was found after the reflection of the pulse at the wet-dry sand interface (E and F). The points G and H showing small upward shift on the first derivative might be the actual points of inflection after final reflection of the pulse at the end of the sensor. Selection of the inflection points at E and F reduced L_a in Eq.(1), consequently resulting in underestimation of ε and θ as similar to Expt.1.1 in Fig. 3. Although the waveform was generated from a part of the sensor within the wet sand, the entire length of the sensor (0.1 m) was used in calculating ε according to Eq.(1). There still remains scope to improve the programs for analyzing this type of irregular-shaped waveforms. One such possibility is to use a short-circuited sensor at the end, which could result in a sharp downward shift of the waveform at the end of the sensor. In case of θ_{dry} = 0.25 $m^3 m^{-3}$ (Expt.2.3),

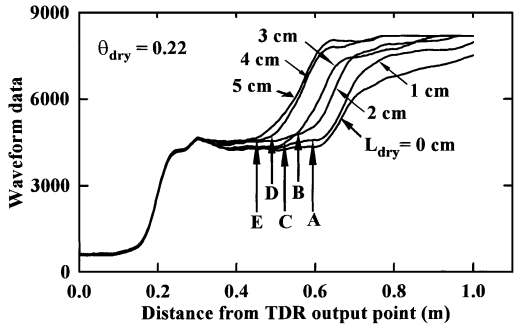

Fig. 6 TDR waveforms for six different thickness of the dry sand layer, Ldry, with ($\theta_{dry}=0.22\,m^3\,m^{-3}$ (Expt. 4).

whereas the waveform did not move up noticeably at the wet-dry sand, it moved up significantly after the major reflection of the pulse from the end of the sensor at point I in Fig.4. The programs selected the appropriate inflection point at J and reasonably estimated ε in this case.

While the reflected pulse moved up considerably at the wet-dry sand interface depending on θ_{dry}, thickness of the dry sand layer, L_{dry}, had virtually no effect on the determination of the reflection point at the end of sensor. For $\theta_{dry}=0.05\,m^3\,m^{-3}$ in Expt.3, the reflected TDR pulse always shifted up considerably at the wet-dry sand interface before the final reflection from the end of the sensor regardless of L_{dry} values. Fig.5 presents four waveforms in Expt.3 where A, B, and C show the approximate locations of reflection of the TDR pulse at the wet-dry sand interface. As can be viewed from the shape of the waveforms, the reflection of the pulse from the end of the sensor could not be identified since the major reflections occurred at A, B, and C. As a result, the inflection of the waveform at the wet-dry sand interface, as similar to Expt.2.1 and Expt.2.2, the programs underestimated ε and θ.

Fig. 6 shows six waveforms for $\theta_{dry}=0.22\,m^3\,m^{-3}$ in Expt.4. The inflection of the waveform always occurred after the final reflection at the end of the sensor regardless of L_{dry} values as it occurred for $\theta_{dry}=0.25\,m^3\,m^{-3}$ in Expt.2.3. The dry sand layer at the bottom could not change the major inflection point regardless of its thickness in this case. The approximate locations of reflection at the wet-dry interface occurred at A, B, C, D, and E in Fig. 6. Since the reflected pulse at the wet-dry interface did not move up considerably, the programs properly interpreted the waveforms and accurately estimated ε and hence θ in Expt. 4 for all values of L_{dry}.

4. 2. Transverse Heterogeneity between Two Rods of the Sensor

TDR underestimated ε in all twelve measurements of Expt.5 depending on : (i) the volume of the dry sands within the sampled volume of the sensor, and (ii) whether the core wire or the shield wire of the sensor was in the dry sand. Table 2 lists the results of twelve measurements in Expt.5. TDR sensor sampled a cylindrical volume of soil with length equal to the length of the sensor and diameter approximately 1.4 times the spacing of the wires (Zegellin *et al*., 1989). The sampling volumes of dry and wet sands were adjusted by changing the relative position of the sensor from the partition (Expt.5.9–5.11 in Table 2). Underestimation of ε and θ increased as the sampling dry sand volume increased.

Because of the low ε of dry sand the TDR pulse traveled faster than in the wet sand (Lorrain and Corson, 1970). The pulse reflected earlier from the wire inserted in the dry sand than from the wire inserted in the wet sand. Fig. 7 demonstrates the influence of two different speeds of the pulse in the core and shield wires on the waveforms of Expt.5.1 (Table 2). The final points of inflection (C and D) and hence the final points of reflection (A and B) were different for these two waveforms. The path of travel of the pulse L_a in Eq.(1) was shorter when the core wire was in dry sand than in wet sand. The mutual interchange of the two wires of the sensor in the dry and wet portions of the same sample resulted in two different ε (Table 2). Since intensity of the electrical potential was much higher around

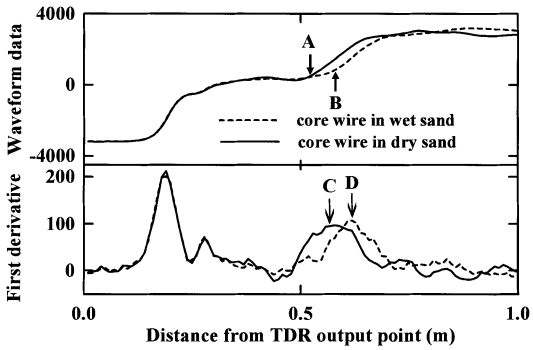

Fig. 7 TDR waveforms and their first derivatives for different positions of the two wires of the sensor in a transverse heterogeneous water profile (Expt. 5.1).

the core wire than around the shield wire (Zegelin *et al*., 1989), TDR exerted greater weight around the core wire than around the shield wire. This resulted in higher ε when the core wire was in wet sand than in dry sand.

5. Conclusions

The TDR-support softwares located the initial and final points of reflection of the TDR pulse on the waveform using its first derivative to calculate the dielectric constant, ε, based on the distance between these points. When a dry sand was at the bottom TDR, waveforms shifted up to some extent at the wet-dry sand interface depending on the water content of the dry layer, θ_{dry}. In case of $\theta_{dry}=0.05$ and 0.15 $m^3 m^{-3}$, the early upward shift of the waveform was much higher. The maximum first derivative occurred after the reflection of the pulse at the wet-dry sand interface. The programs analyzed only part of the waveform that resulted in underestimation of ε and θ. For $\theta_{dry}=0.22\,m^3 m^{-3}$, the magnitude of this upward shift was insignificant. The algorithms of the programs correctly estimated the travel path of the pulse L_a in Eq.(1). The major inflection point on the waveform located at the maximum first derivative occurred after the final reflection of the pulse at the end of the sensor.

Thickness of the bottom dry sand layer, L_{dry}, had no effect on the wave analysis. When the bottom layer was relatively wet ($\theta_{dry}=0.22\,m^3 m^{-3}$), the program algorithms selected the final inflection of the waveform after the pulse reflected back from the end of the sensor regardless of L_{dry} values providing the correct measurement of ε and θ. On the other hand, the inflection point was selected just after the pulse reflected back at the wet-dry sand interface for all values of L_{dry} for quite low θ_{dry} ($=0.05\,m^3 m^{-3}$), resulting in underestimation in ε and θ.

In case of soil-water heterogeneity in the direction transverse along the sensor, the TDR pulse traveled faster through the wire of the sensor inserted in the dry sand than through the wire inserted in the wet sand. The early reflection of the pulse in the dry sand shortened its path of travel and TDR always underestimated ε and θ regardless of the position of the two wires of the sensor. The degree of underestimation was higher when the core wire of the sensor was in dry sand.

Acknowledgement

The principal author is an Associate Professor of the department of Irrigation and Water Management of the Bangladesh Agricultural University (BAU), Mymensingh-2202. This research was conducted at Saga University using the funding of Japan Society for Promotion of Science (JSPS). We sincerely acknowledge the JSPS and the BAU authorities for their support.

References

Baker, J.M. and Allmaras, R.R. (1990) : System for automating and multiplexing soil moisture measurement by time-domain reflectometry. Soil Sci. Soc. Am. J., **54** : 1-6.

Dasberg, S. and Hopmans, J.W. (1992) : Time-domain reflectometry calibration for uniformly and non-uniformly wetted sandy and clayey loam soils. Soil Sci. Soc. Am. J., **56** : 1341-1345.

Davis, J.L. and Chudobiak, W.J. (1975) : In situ meter for measuring relative permittivity of soils. Paper 75-1A. Geological Survey of

Canada. Energy, Mines, and Resources of Canada, Ottawa.

Evett, S.R. (1998) : The TACQ computer program for automatic measurement of water content and bulk electrical conductivity using time domain reflectometry. Paper no.983182, presented at the Annual International Meeting of ASAE, Orlando, Florida, July 12–15, 1998.

Heimovaara, T.J. and Bouten, W. (1990) : A computer-controlled 36-channel time domain reflectometry system for monitoring soil water contents. Water Resour. Res., **26** : 2311–2316.

Hokett, S.L., Chapman, J.B. and Cloud, S.D. (1992) : Time-domain reflectometry response to lateral soil-water content heterogeneities. Soil Sci. Soc. Am. J., **56** : 313–316.

Lorrain, P. and Corson, D.R.. (1970) : Electromagnetic fields and waves (2nd ed.). W. H. Freeman, New York.

Nadler, A.S., Dasberg, S. and Lapid, I. (1991) : Time domain reflectometry measurements of water content and electrical conductivity of layered soil columns. Soil Sci. Soc. Am. J., **55** : 938–943.

Or, D., Fisher, B., Hubscher, R.A. and Wraith J. (1999) : WinTDR99. Users guide. Utah State University, Utah, USA.

Tektronix. (1990) : 1502C metallic time-domain reflectometer : operator manual. Tektronix, Inc. Beaverton, OR97077, USA.

Topp, G.C., Davis, J.L. and Annan, A.P. (1980) : Electromagnetic determination of soil-water content : measurements in coaxial transmission lines. Water Resour. Res., **16** : 574–582.

Topp, G.C., Davis, J.L. and Annan, A.P. (1982) : Electromagnetic determination of soil water content using TDR : I. Applications to wetting fronts and steep gradients. Soil Sci. Soc. Am. J., **46** : 672–678.

Zegelin, S.J., White, I. and Jenkins, D.R. (1989) : Improved field probes for soil-water content and electrical conductivity measurement using time-domain reflectometry. Water Resour. Res., **25** : 2367–2376.

不均一な土壌水分分布が TDR 土壌水分測定値に及ぼす影響について

M. A. Mojid・取出伸夫・長　裕幸
佐賀大学農学部
840–8502 佐賀市本庄町 1 番地

要　　旨

TDR を用いて土壌水分量を推定する際，水分分布が不均一な条件下で測定される波形と市販の波形解析プログラムとの適用条件について検討を行った。砂層において先端部が乾燥している場合，計算されるパルスの反射ポイントは乾湿層間の境界面で発生する反射波の影響を受け，プローブの先端との間にずれを生じることが分かった。湿潤土層の水分量 $\theta_{wet}=0.29\,m^3\,m^{-3}$ に対し乾燥土層の水分量 θ_{dry} が $0.15\,m^3\,m^{-3}$ 以下では，プログラムは不正確な反射ポイントを示し，水分量を過小に推定した。θ_{dry} が $0.22\,m^3\,m^{-3}$ になると反射ポイントの違いの影響は小さくなり，プログラムはほぼ正確な値を示した。乾燥層の厚さの違いは水分量の違いに比べて，波形に与える影響は小さかった。しかし，乾燥層の水分量が非常に小さくなると（$\theta_{dry}=0.05\,m^3\,m^{-3}$），厚さに関係なく反射ポイントは乾湿層境界面で与えられ，水分量は過小に計算された。

プローブにおける 2 本のロッド間で水分量が異なる場合，プログラムは水分量を常に過小に計算した。さらにコア部のロッドが乾燥側にある場合，その差は大きくなることが分かった。

キーワード：TDR，土壌水分分布，縦方向の不均一性，横方向の不均一性，波形解析

受稿年月日：2000 年 4 月 13 日
受理年月日：2002 年 1 月 24 日